AIMS Mathematics, 11(3): 8635–8654.
DOI: 10.3934/math.2026355
Received: 06 January 2026
Revised: 19 March 2026
Accepted: 23 March 2026
Published: 31 March 2026

https://www.aimspress.com/journal/Math

Research article

Applications of two sufficient descent spectral conjugate gradient methods in image denoising

Yu Cai[1], **Hong Yue**[2] **and Chenyun Mo**[1,*]

[1] School of Education, Huaibei Institute of Technology, Huaibei 235000, Anhui, China

[2] Department of Basic Courses, Liaoning Finance and Trade College, Xingcheng 125105, Liaoning, China

* **Correspondence:** Email: 15956510540@163.com.

Abstract: To solve large-scale unconstrained optimization problems, this paper further investigated the RMIL conjugate gradient method and its variants in order to propose two new spectral conjugate gradient methods. Under basic assumptions for unconstrained optimization problems, where the level set was bounded and the gradient was Lipschitz continuous, the search directions generated by the proposed methods satisfied the sufficient descent property independent of the choice of line search. Moreover, the global convergence of the methods was established under both the standard Wolfe line search and the standard Armijo line search. Numerical experiments on unconstrained optimization and image denoising problems under both line searches demonstrated that the two proposed spectral conjugate gradient methods exhibited superior performance and broader applicability.

Keywords: unconstrained optimization; spectral conjugate gradient methods; sufficient descent property; global convergence; image denoising
Mathematics Subject Classification: 65K10, 68U10, 90C30

1. Introduction

The conjugate gradient method is widely used to solve the following unconstrained optimization problem

$$\min f(x),\ x \in \mathbb{R}^n, \tag{1.1}$$

where $f : \mathbb{R}^n \to \mathbb{R}$ is a continuously differentiable function. In 1952, Hestenes and Stiefel [1] first introduced the linear conjugate gradient method for solving systems of linear equations with symmetric positive definite matrices. Later in 1964, Fletcher and Reeves [2] extended this method for solving nonlinear unconstrained optimization problems, which is generally regarded as the beginning

of nonlinear conjugate gradient methods. The general iterative scheme of the conjugate gradient method can be expressed in the following form:

$$x_{k+1} = x_k + \alpha_k d_k \tag{1.2}$$

and

$$d_k = \begin{cases} -g_k, & k = 1, \\ -g_k + \beta_k d_{k-1}, & k \geq 2, \end{cases} \tag{1.3}$$

where $g_k := \nabla f(x_k)$, $\alpha_k > 0$ is the step length determined by a line search, d_k is the search direction, and β_k is the conjugate parameter. It is well known that different choices of β_k give rise to different conjugate gradient methods. The classical conjugate gradient methods include the Hestenes-Stiefel (HS) method [1], the Fletcher-Reeves (FR) method [2], the Polak-Ribière-Polyak(PRP) method [3, 4], and the Dai-Yuan (DY) method [5]. Their corresponding conjugate parameters are defined as follows:

$$\beta_k^{\mathrm{HS}} = \frac{g_k^T y_{k-1}}{d_{k-1}^T y_{k-1}}, \ \beta_k^{\mathrm{FR}} = \frac{\|g_k\|^2}{\|g_{k-1}\|^2}, \ \beta_k^{\mathrm{PRP}} = \frac{g_k^T y_{k-1}}{\|g_{k-1}\|^2}, \ \beta_k^{\mathrm{DY}} = \frac{\|g_k\|^2}{d_{k-1}^T y_{k-1}},$$

where $y_{k-1} = g_k - g_{k-1}$ and $\|\cdot\|$ denotes the Euclidean norm of vectors. In particular, when the objective function is quadratic and exact line search is employed, the aforementioned four methods are equivalent. Extensive research has shown that the FR and DY methods possess favorable convergence properties, whereas the PRP and HS methods exhibit excellent numerical performance. To develop methods that ensure both good convergence and strong numerical performance, numerous scholars have conducted important research in this area [6–10].

Over the past two decades, significant research on search directions has led to the development of several important variants of the classical conjugate gradient method. Several notable achievements include the three-term conjugate gradient method [11], the spectral conjugate gradient method [12], the spectral three-term conjugate gradient method [13], and the preconditioned conjugate gradient method [14].

On the other hand, conjugate gradient methods have been extended to other domains beyond solving (1.1), such as the Riemannian manifold optimization [15], the tensor optimization [16], and the sparse optimization [17]. It is worthwhile to mention that using the conjugate gradient method to solve the image denoising problems in the sparse optimization has received wide attention. For example, Jiang et al. [18] combined the hybrid conjugate gradient method and the convex combination technique to develop a family of hybrid three-term conjugate gradient methods for salt-and-pepper noise removal. Subsequently, Wang et al. [19] proposed a modified RMIL conjugate gradient-based projection method for constrained nonlinear equations, with applications to image denoising problems. Further related studies can be found in [20–22].

This paper focuses on the spectral conjugate gradient method and its application to image denoising. To this end, we introduce two new spectral conjugate gradient methods by extending the RMIL method [23] and the MRMIL method [24], respectively. The proposed methods reduce to the RMIL method under the exact line search. In addition, they generate search directions d_k that guarantee the sufficient descent property independently of any line search. Notably, we establish global convergence under both the standard Wolfe and Armijo line searches. Comprehensive

numerical experiments on unconstrained optimization and image denoising problems, conducted under both line searches, consistently demonstrate the reliability and superiority of the proposed methods.

The remainder of this paper is structured as follows. Section 2 details the motivation and algorithms of the two proposed spectral conjugate gradient methods. The global convergence properties of both methods under the standard Wolfe and Armijo line search conditions are established in Section 3. Finally, Sections 4 and 5 present numerical results that demonstrate the effectiveness and efficiency of the proposed methods on unconstrained optimization and image denoising problems, respectively.

2. Motivation and algorithms

Rivaie et al. [23] proposed a new conjugate parameter, defined by

$$\beta_k^{\mathrm{RMIL}} = \frac{g_k^T(g_k - g_{k-1})}{\|d_{k-1}\|^2}, \tag{2.1}$$

and established its global convergence under the exact line search. Similar to the β_k^{PRP}, if a small step size is produced in one iteration, the search direction in the subsequent iteration automatically approaches the negative gradient direction, thereby inheriting the restart property. Subsequently, Rivaie et al. [24] further modified the β_k^{RMIL} as follows:

$$\beta_k^{\mathrm{MRMIL}} = \frac{g_k^T(g_k - g_{k-1} - d_{k-1})}{\|d_{k-1}\|^2}, \tag{2.2}$$

It can be observed that if the exact line search is used, the condition $g_k^T d_{k-1} = 0$ holds, which renders (2.1) equivalent to (2.2). They analyzed and discussed the sufficient descent property and global convergence of the MRMIL method under the strong Wolfe line search.

In recent years, the parameters β_k^{RMIL} and β_k^{MRMIL} have attracted considerable research interest. For instance, Yousif [25] proposed the following conjugate parameter

$$\beta_k^{\mathrm{RMIL+}} = \begin{cases} \dfrac{g_k^T(g_k - g_{k-1})}{\|d_{k-1}\|^2}, & \text{if } 0 \le g_k^T g_{k-1} \le \|g_k\|^2, \\ 0, & \text{otherwise.} \end{cases}$$

Subsequently, another modified version of the RMIL parameter was proposed in [26], defined as

$$\beta_k^{\mathrm{RMIL^*}} = \begin{cases} \dfrac{g_k^T(g_k - g_{k-1})}{\|d_{k-1}\|^2}, & \text{if } |g_k^T g_{k-1}| \le \|g_k\|^2, \\ 0, & \text{otherwise.} \end{cases}$$

References [25, 26] have established the global convergence of their relevant conjugate gradient methods under the strong Wolfe line search and the exact line search, respectively. Nevertheless, the global convergence properties of the parameters defined by (2.1) and (2.2) under the standard Wolfe or Armijo line search conditions have received considerably less attention. This paper bridges the gap by integrating these parameters into a spectral conjugate gradient method. In the following, we introduce some fundamental concepts of spectral conjugate gradient methods.

Birigin and Martínez [27] combined the spectral gradient method with the conjugate gradient method to propose the spectral conjugate gradient method, and they generalized the iterative scheme of (1.3) into the following form:

$$d_k = \begin{cases} -g_k, & k = 1, \\ -\theta_k g_k + \beta_k d_{k-1}, & k \geq 2, \end{cases} \tag{2.3}$$

where

$$\beta_k = \frac{g_k^T(\theta_k y_{k-1} - s_{k-1})}{d_{k-1}^T y_{k-1}}, \quad \theta_k = \frac{s_{k-1}^T s_{k-1}}{s_{k-1}^T y_{k-1}}, \quad s_{k-1} = x_k - x_{k-1}.$$

In this formulation, θ_k is referred to as the spectral parameter and β_k is regarded as the conjugate parameter. Although this spectral conjugate gradient method exhibits satisfactory numerical performance in practical computations, it gives no guarantee of the descent property in its search direction.

Zhang et al. [28] proposed a spectral FR conjugate gradient method by combining the FR conjugate gradient method with (2.3), and the search direction is given by

$$d_k = \begin{cases} -g_k, & k = 1, \\ -(1 + \beta_k \frac{g_k^T d_{k-1}}{\|g_k\|^2}) g_k + \beta_k d_{k-1}, & k \geq 2, \end{cases} \tag{2.4}$$

where

$$\beta_k = \beta_k^{FR} = \frac{\|g_k\|^2}{\|g_{k-1}\|^2}.$$

It is straightforward to verify that the search direction d_k defined in (2.4) satisfies the sufficient descent condition

$$g_k^T d_k = -\|g_k\|^2 \tag{2.5}$$

for any choice of the parameter β_k.

Although (2.1) and (2.2) have attracted considerable attention, the resulting search directions are not guaranteed to be descent directions under inexact line searches. To overcome this limitation, we construct the search direction d_k in two ways: one way combines the search direction defined in (2.4) with (2.1), and the other way combines the search direction defined in (2.4) with (2.2). This construction yields two spectral conjugate gradient methods whose directions satisfy the sufficient descent property independent of the line search. Specifically, the method incorporating (2.1) is referred to as the SRMIL method, whereas the method incorporating (2.2) is referred to as the SMRMIL method. To establish the global convergence of the proposed methods, we adopt the standard Wolfe line search, where the step length α_k satisfies

$$\begin{cases} f(x_k + \alpha_k d_k) \leq f(x_k) + \rho \alpha_k g_k^T d_k, \\ g(x_k + \alpha_k d_k)^T d_k \geq \sigma g_k^T d_k, \end{cases} \tag{2.6}$$

where $0 < \rho < \sigma < 1$, and the standard Armijo line search, where $\alpha_k = \delta^j$ with $\delta \in (0, 1)$ and the smallest integer $j \geq 0$ such that

$$f(x_k + \alpha_k d_k) \leq f(x_k) + \rho \alpha_k g_k^T d_k. \tag{2.7}$$

(2.7) coincides with the first inequality in (2.6), whereas the Wolfe line search additionally requires the curvature condition.

In the following, we present the algorithmic frameworks of the SRMIL and SMRMIL methods under the standard Wolfe or Armijo line search.

Algorithm 1 The SRMIL and SMRMIL methods under the Wolfe or Armijo line search

Step 0. Select an initial point $x_1 \in \mathbb{R}^n$ and parameters $\rho, \delta, \sigma \in (0, 1)$. Given termination tolerance $\epsilon > 0$, set $d_1 := -g_1$, and let $k := 1$.
Step 1. If $\|g_k\| \leq \epsilon$, then stop.
Step 2. Compute the step size α_k using either:
(i) the standard Wolfe line search (2.6), or
(ii) the standard Armijo line search (2.7).
Step 3. Update the next iterate by (1.2).
Step 4. Choose the conjugate parameter β_{k+1} using either (2.1) or (2.2), and then calculate the search direction d_{k+1} by (2.4)
Step 5. Set $k := k + 1$, and return to Step 1.

3. Convergence analysis

To establish the global convergence of the SRMIL and SMRMIL methods under the standard Wolfe and Armijo line searches, we introduce two basic assumptions about the objective function in this section.

(A1) The level set $\Omega = \{x \in \mathbb{R}^n | f(x) \leq f(x_1)\}$ of the objective function $f(x)$ is bounded, namely, there exists a constant $B > 0$ such that

$$\|x\| \leq B, \quad \forall\, x \in \Omega. \tag{3.1}$$

(A2) In some neighborhood U of the level set Ω, the gradient function $g(x)$ is Lipschitz continuous, that is, there exists a constant $L > 0$ satisfying

$$\|g(y) - g(x)\| \leq L\|y - x\|, \quad \forall\, x, y \in U. \tag{3.2}$$

From assumptions (A1) and (A2), it follows that the gradient norm is bounded on Ω, which implies the existence of a constant $\overline{\gamma}$ such that

$$\|g(x)\| \leq \overline{\gamma}, \quad \forall\, x \in \Omega. \tag{3.3}$$

As the sufficient descent condition (2.5) is always satisfied for both the SRMIL and SMRMIL methods, we can derive the following fundamental inequality:

$$\|d_k\| \geq \|g_k\|, \quad \forall\, k \geq 1, \tag{3.4}$$

This inequality plays a crucial role in the subsequent convergence analysis.

The global convergence of conjugate gradient methods is established through the Zoutendijk condition, which was originally introduced by Wolfe [29] and Zoutendijk [30] under the standard Wolfe line search. The following lemma shows that an alternative form of this condition holds for the proposed methods under both the standard Wolfe and Armijo line searches.

Lemma 3.1. *Under Assumptions (A1) and (A2), consider the iterative schemes* (1.2) *and* (1.3)*, where the search direction d_k satisfies the sufficient descent condition* (2.5) *and the step length α_k is determined by either the standard Wolfe line search* (2.6) *or the standard Armijo line search* (2.7)*. Then the following inequality holds:*

$$\sum_{k\geq 1} \frac{\|g_k\|^4}{\|d_k\|^2} < +\infty. \tag{3.5}$$

Proof. We now discuss the two cases separately, depending on whether α_k is determined by either the standard Wolfe or the standard Armijo line search.

Case I: Suppose that α_k is determined by the standard Wolfe line search. The second inequality in (2.6) gives

$$(g_{k+1} - g_k)^T d_k \geq (\sigma - 1) g_k^T d_k.$$

On the other hand, the Lipschitz condition (3.2) indicates

$$(g_{k+1} - g_k)^T d_k \leq L\alpha_k \|d_k\|^2.$$

Combining both inequalities leads to

$$\alpha_k \geq \frac{\sigma - 1}{L} \frac{g_k^T d_k}{\|d_k\|^2}.$$

Together with the sufficient descent condition (2.5) and the first inequality of the Wolfe condition (2.6), these imply that (3.5) holds.

Case II: Suppose that α_k is determined by the standard Armijo line search, and we consider the following two situations separately.

(i) if $\alpha_k = 1$, inequality (3.4) indicates

$$\alpha_k \geq \frac{\|g_k\|^2}{\|d_k\|^2}.$$

(ii) if $\alpha_k < 1$, then $\frac{\alpha_k}{\delta}$ does not satisfy (2.7); hence, we conclude that

$$f(x_k + \frac{\alpha_k}{\delta} d_k) - f(x_k) > \rho \frac{\alpha_k}{\delta} g_k^T d_k.$$

Applying the mean value theorem and (3.2), there exists $t \in (0, 1)$ such that

$$\begin{aligned} f(x_k + \frac{\alpha_k}{\delta} d_k) - f(x_k) &= \frac{\alpha_k}{\delta} g(x_k + t\frac{\alpha_k}{\delta} d_k)^T d_k \\ &= \frac{\alpha_k}{\delta} g_k^T d_k + \frac{\alpha_k}{\delta} (g(x_k + t\frac{\alpha_k}{\delta} d_k) - g_k)^T d_k \\ &\leq \frac{\alpha_k}{\delta} g_k^T d_k + L\frac{\alpha_k^2}{\delta^2} \|d_k\|^2. \end{aligned}$$

Combining the preceding inequalities with the sufficient descent condition (2.5) yields

$$\alpha_k \geq \frac{\delta(\rho - 1) g_k^T d_k}{L\|d_k\|^2} = \frac{\delta(1 - \rho)\|g_k\|^2}{L\|d_k\|^2}.$$

From the analysis of (i) and (ii), we obtain the following unified lower bound for α_k:

$$\alpha_k \geq c\frac{\|g_k\|^2}{\|d_k\|^2},$$

where

$$c = \min\left\{1, \frac{\delta(1-\rho)}{L}\right\}.$$

Together with (2.5) and the Armijo condition (2.7), these results imply that (3.5) holds, thereby completing the proof of the lemma. □

The preceding lemma guarantees that (3.5) holds under the sufficient descent condition (2.5), regardless of whether step length α_k is determined by the standard Wolfe (2.6) or Armijo (2.7) line search. This result serves as a foundation for the global convergence of the SRMIL and SMRMIL methods.

Theorem 3.1. *Consider the sequences $\{x_k\}$ and $\{d_k\}$ generated by the proposed methods. If Assumptions (A1) and (A2) are satisfied, then we have*

$$\liminf_{k\to\infty} \|g_k\| = 0.$$

Proof. We prove by contradiction. Suppose that there exists a constant $\gamma > 0$ such that

$$\|g_k\| \geq \gamma, \quad \forall\, k \geq 1. \tag{3.6}$$

Accordingly, the subsequent analysis is divided into two cases corresponding to the SRMIL and SMRMIL methods.

Case I (SRMIL) For $k \geq 2$, it follows from (2.4) that

$$\begin{aligned}\|d_k\| &\leq \|g_k\| + |\beta_k|\frac{\|g_k\|\|d_{k-1}\|}{\|g_k\|^2}\|g_k\| + |\beta_k|\|d_{k-1}\| \\ &= \|g_k\| + 2|\beta_k|\|d_{k-1}\|. \end{aligned} \tag{3.7}$$

Combining this inequality with (2.1), (3.3), (3.4), and (3.6), we have

$$\begin{aligned}\|d_k\| &\leq \|g_k\| + 2\frac{|g_k^T(g_k - g_{k-1})|}{\|d_{k-1}\|^2}\|d_{k-1}\| \\ &\leq \|g_k\| + 2\frac{\|g_k\|\|g_k - g_{k-1}\|}{\|d_{k-1}\|\|g_{k-1}\|}\|d_{k-1}\| \\ &\leq \|g_k\| + 2\frac{\|g_k\|(\|g_k\| + \|g_{k-1}\|)}{\|g_{k-1}\|} \\ &\leq \overline{\gamma} + \frac{4\overline{\gamma}^2}{\gamma} \triangleq M_1. \end{aligned} \tag{3.8}$$

Case II (SMRMIL) Comparing (2.1) and (2.2), we find that

$$|\beta_k^{MRMIL}| \leq |\beta_k^{RMIL}| + \frac{|g_k^T d_{k-1}|}{\|d_{k-1}\|^2} \leq |\beta_k^{RMIL}| + \frac{\|g_k\|}{\|d_{k-1}\|}.$$

By following the same reasoning as in Case I and applying the above inequality together with (3.3), (3.7), and (3.8) for all $k \geq 2$, we obtain

$$\begin{aligned} \|d_k\| &\leq \|g_k\| + 2|\beta_k^{MRMIL}|\|d_{k-1}\| \\ &\leq \|g_k\| + 2|\beta_k^{RMIL}|\|d_{k-1}\| + 2\frac{\|g_k\|}{\|d_{k-1}\|}\|d_{k-1}\| \\ &\leq M_1 + 2\overline{\gamma} \triangleq M_2. \end{aligned}$$

To summarize, we have established the uniform bound $\|d_k\| \leq M_2$ for all $k \geq 1$ in both the SRMIL and SMRMIL methods. In conjunction with the gradient bound (3.6), this yields

$$\sum_{k=1}^{\infty} \frac{\|g_k\|^4}{\|d_k\|^2} \geq \sum_{k=1}^{\infty} \frac{\gamma^4}{M_2^2} = +\infty.$$

This result contradicts the Zoutendijk condition (3.5), thereby completing the proof of the theorem. □

4. Unconstrained optimization problems

In order to demonstrate the effectiveness of the SRMIL and SMRMIL methods under both the standard Wolfe and Armijo line searches, we apply them to solve unconstrained optimization problems. For comparison, the following representative methods are selected: the MRMIL method [24], the RMIL method [23], and the well-known HZ method [7].

The numerical experiments are conducted on two test sets, each consisting of 82 unconstrained optimization problems taken from [31, 32]. The first set was tested under the standard Wolfe line search, while the second set was tested under the standard Armijo line search. The dimensions of the test problems are set to 120, 1200, and 12000. For the standard Wolfe line search, the parameters were set to $\rho = 0.01$ and $\sigma = 0.1$. For the standard Armijo line search, the parameters were set to $\delta = 0.5$ and $\rho = 0.2$. The complete numerical comparison tables are provided in the GitHub repository: `https://github.com/fenhyu/paper-tables`. The algorithm terminates when either $\|g_k\| \leq 10^{-6}$ or Itr > 10000. A run is recorded as "F" if the stopping condition Itr > 10000 is reached. All experiments were performed in MATLAB R2020a on a Dell computer with an Intel Core i9-12900H processor and 32 GB of RAM.

It is worth noting that, under both the standard Wolfe and Armijo line searches, we compare the five methods in terms of four performance metrics, namely, the number of iterations (Itr), the CPU computing time (Tcpu), the number of function evaluations (N_f), and the number of gradient evaluations (N_g). Furthermore, we employ the performance profiles of Dolan and Moré [33] to visually compare the performance in terms of Itr, Tcpu, N_f, and N_g. The results obtained under the standard Wolfe line search (Figures 1–4) and Armijo line search (Figures 5–8) are presented separately.

In the Dolan-Moré performance profile, a higher curve indicates better overall performance of the solver. As shown by the performance profiles under the standard Wolfe line search (Figures 1–4), the proposed SMRMIL and SRMIL methods exhibit overall superior performance among the five methods in terms of Itr, Tcpu, N_f, and N_g. Specifically, they successfully solve approximately 90% of the test problems within a performance ratio when $\tau = 3$, whereas the MRMIL, RMIL, and HZ

methods solve only about 85%. Under the standard Armijo line search (Figures 5–8), the proposed methods remain highly competitive across the same four metrics, and their advantages are again evident from the corresponding performance profiles. Furthermore, under the Armijo line search, the performance profiles confirm that both the SMRMIL and SRMIL methods successfully solve about 95% of the test problems when $\tau \approx 3$, whereas the MRMIL, RMIL, and HZ methods solve fewer than 90% of the problems at the same performance ratio. Overall, the SMRMIL and SRMIL methods demonstrate higher effectiveness in solving large-scale unconstrained optimization problems under both the standard Wolfe and Armijo line searches.

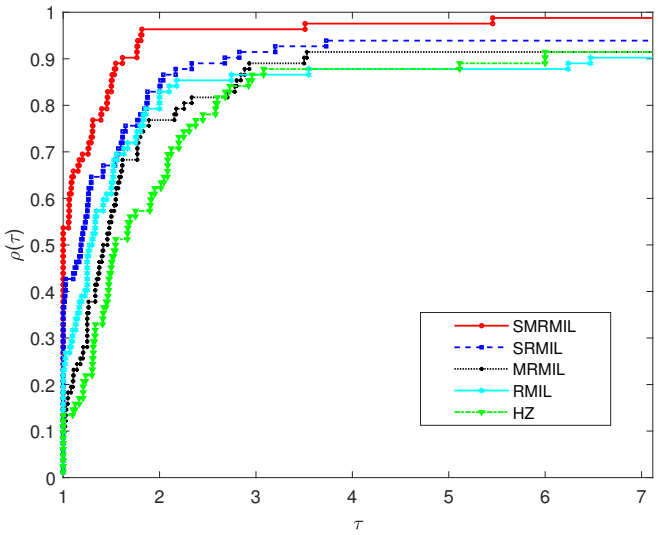

Figure 1. Performance profile of Itr under the standard Wolfe line search.

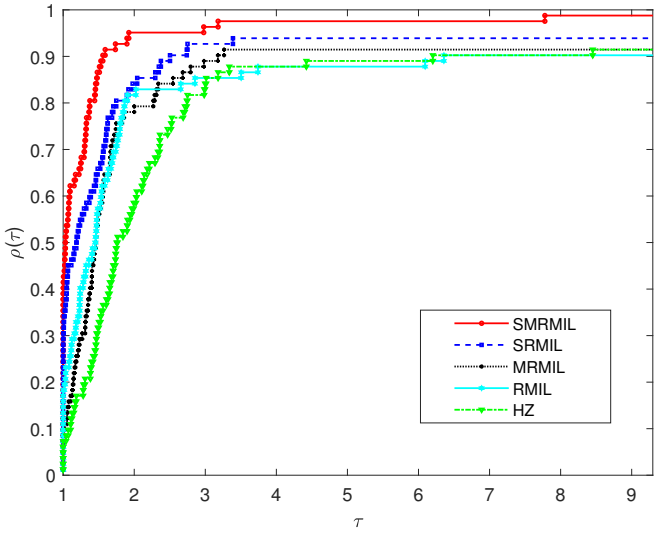

Figure 2. Performance profile of Tcpu under the standard Wolfe line search.

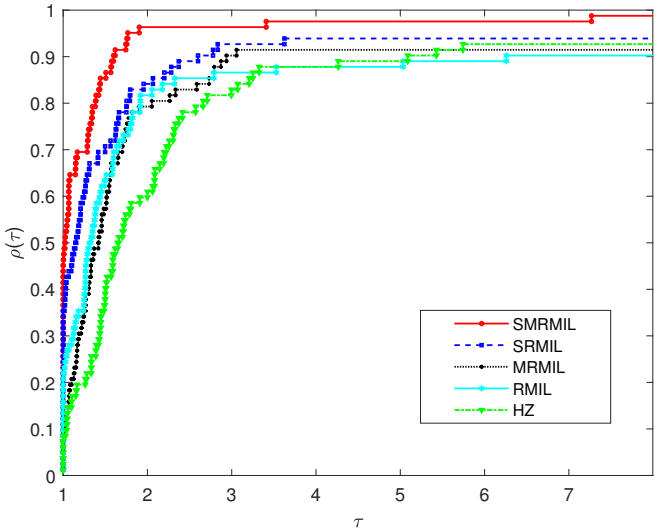

Figure 3. Performance profile of N_f under the standard Wolfe line search.

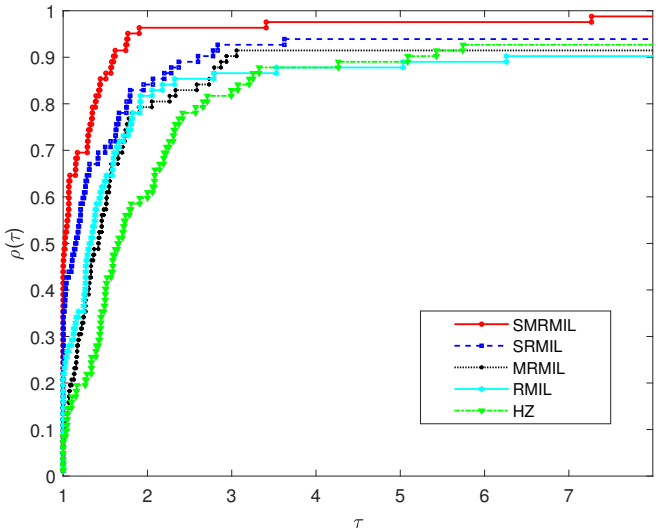

Figure 4. Performance profile of N_g under the standard Wolfe line search.

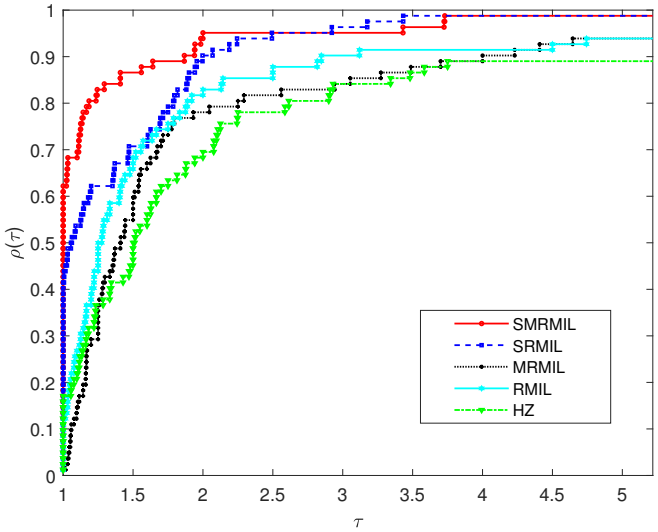

Figure 5. Performance profile of Itr under the standard Armijo line search.

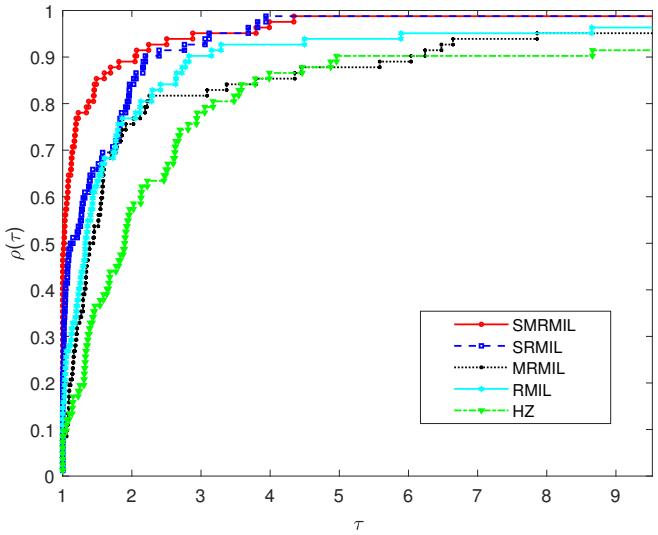

Figure 6. Performance profile of Tcpu under the standard Armijo line search.

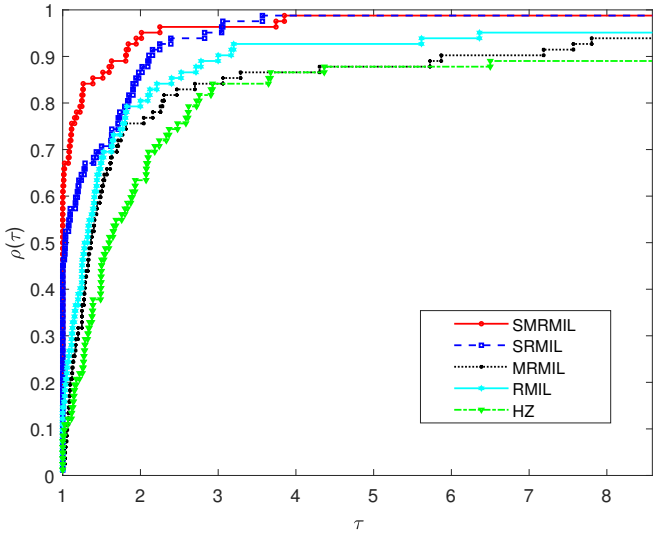

Figure 7. Performance profile of N_f under the standard Armijo line search.

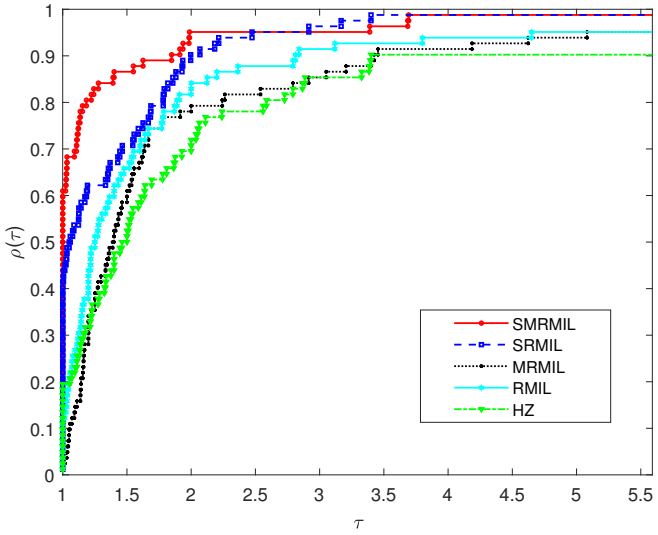

Figure 8. Performance profile of N_g under the standard Armijo line search.

5. Image denoising problems

Image denoising plays a vital role in image processing, aiming to remove noise from corrupted images while preserving the original features and edge structures. Among various types of image noise, salt-and-pepper noise is one of the most common. It is typically caused by malfunctioning sensors, transmission errors, or storage corruption, and appears as randomly distributed white and black pixels. To demonstrate the broad applicability of the SRMIL and SMRMIL methods, we further apply them to the task of image denoising, specifically for the removal of salt-and-pepper noise.

Raymond et al. [34] proposed a two-stage approach to restore images corrupted by salt-and-pepper noise. In the first stage, an adaptive median filter is employed to detect noisy pixels. Consider an

original image X of size $M \times N$, with its index set defined as $\mathscr{A} = \{1, 2, \ldots, M\} \times \{1, 2, \ldots, N\}$, where $x_{i,j}$ denotes the pixel value at location (i, j). Let $\mathscr{N} \subset \mathscr{A}$ denote the index set of noisy pixels detected in the first stage, and $|\mathscr{N}|$ the number of elements in $\mathscr{N}$. The set of four neighboring points of pixel (i, j) is denoted by $\mathscr{V}_{i,j} = \{(i, j-1), (i, j+1), (i-1, j), (i+1, j)\}$. In the second stage, the noisy pixels are restored by minimizing the following nonsmooth unconstrained function:

$$\min_u F_\alpha(u) = \sum_{(i,j)\in\mathscr{N}} \left[|u_{i,j} - x_{i,j}| + \tfrac{\beta}{2}(2S^1_{i,j} + S^2_{i,j}) \right], \tag{5.1}$$

where

$$S^1_{i,j} = \sum_{(m,n)\in\mathscr{V}_{i,j}\setminus\mathscr{N}} \varphi_\alpha(u_{i,j} - x_{m,n}), \quad S^2_{i,j} = \sum_{(m,n)\in\mathscr{V}_{i,j}\cap\mathscr{N}} \varphi_\alpha(u_{i,j} - u_{m,n}),$$

$\varphi_\alpha(t) = \sqrt{t^2 + \alpha}$ $(\alpha > 0)$ is an edge-preserving potential function, and β is a regularization parameter. The vector $u = [u_{i,j}]_{(i,j)\in\mathscr{N}}$ is arranged in lexicographic order and has length $|\mathscr{N}|$.

Minimizing the nonsmooth objective function (5.1) is relatively difficult to accomplish exactly. To overcome this challenge, Cai et al. [35] eliminated the data fidelity term $|u_{i,j} - x_{i,j}|$ and proposed to minimize the following smooth unconstrained function:

$$\min_u F_\alpha(u) = \sum_{(i,j)\in\mathscr{N}} \left(2 \sum_{(m,n)\in\mathscr{V}_{i,j}\setminus\mathscr{N}} \varphi_\alpha(u_{i,j} - x_{m,n}) + \sum_{(m,n)\in\mathscr{V}_{i,j}\cap\mathscr{N}} \varphi_\alpha(u_{i,j} - u_{m,n}) \right). \tag{5.2}$$

Subsequent research has focused on integrating conjugate gradient methods with this formulation to effectively address salt-and-pepper noise, as demonstrated in [36–39].

In this section, we apply the SMRMIL, SRMIL, MRMIL, RMIL, and HZ methods to image denoising problems under both the standard Wolfe and Armijo line searches, using the same line search parameters and MATLAB environment as before. First, an adaptive median filter is applied to detect noisy pixels, after which restoration is performed by minimizing (5.2). Five benchmark images are selected for testing: lena (512×512), hill (512×512), boat (512×512), barbara (512×512), and peppers (256×256). Each image is corrupted by salt-and-pepper noise with four different noise ratios: 0.2, 0.4, 0.6, and 0.8. The stopping criterion for this experiment differs from that in the previous section and is satisfied when either of the following conditions holds:

$$\text{Itr} > 300 \quad \text{or} \quad \frac{F_\alpha(u_k) - F_\alpha(u_{k-1})}{F_\alpha(u_{k-1})} \le 10^{-4}.$$

Furthermore, we employ the peak signal-to-noise ratio (PSNR, see [40]) to quantitatively evaluate the restoration quality, defined as

$$\text{PSNR} = 10 \log_{10} \left(\frac{255^2}{\frac{1}{MN} \sum_{i,j} \left(x_{i,j} - x^*_{i,j} \right)^2} \right).$$

Here, $x_{i,j}$ and $x^*_{i,j}$ represent the pixel values of the restored and original images, respectively. A higher PSNR value corresponds to better restoration quality.

Figure 9. Image denoising under the standard Wolfe line search. Row 1: Original images; Row 2: Noisy images (salt-and-pepper noise ratio is 0.8); Rows 3–7: Restored images by the SMRMIL, SRMIL, MRMIL, RMIL, and HZ methods, respectively.

Figure 10. Image denoising under the standard Armijo line search. Row 1: Original images; Row 2: Noisy images (salt-and-pepper noise ratio is 0.8); Rows 3–7: Restored images by the SMRMIL, SRMIL, MRMIL, RMIL, and HZ methods, respectively.

The complete numerical tables for the denoising experiments of the five methods are provided in our GitHub repository: `https://github.com/fenhyu/paper-tables`. The tables report Itr, Tcpu, N_f, N_g, and PSNR for noise ratios 0.2, 0.4, 0.6, and 0.8. To conserve space, Figures 9 and 10 present the visual denoising results obtained under the standard Wolfe and Armijo line searches, respectively. Only the original images, the noisy images at noise ratio 0.8, and the corresponding restored images are displayed. Overall, for these five benchmark images, the proposed SMRMIL and SRMIL methods often achieve competitive PSNR values under both the standard Wolfe and Armijo line searches, indicating competitive denoising performance.

6. Conclusions

In this paper, we have proposed two new spectral conjugate gradient methods, namely, SRMIL and SMRMIL, which combine the spectral gradient technique with the RMIL and MRMIL frameworks. The search directions generated by both methods are shown to satisfy the sufficient descent property independently of the line search strategy. Under basic assumptions for unconstrained optimization problems, namely that the level set is bounded and that its gradient is Lipschitz continuous, we have established the global convergence of the proposed methods for both the standard Wolfe and Armijo line searches. Extensive numerical experiments on large-scale unconstrained optimization and image denoising problems have been conducted to evaluate the practical performance. The results show that SRMIL and SMRMIL are competitive and often outperform the comparison methods (MRMIL, RMIL, and HZ) in terms of iterations, CPU time, and the numbers of function and gradient evaluations (N_f and N_g). For image denoising, the proposed methods also tend to yield higher PSNR values, indicating improved restoration quality.

This study also has certain limitations. First, the convergence analysis is established for smooth unconstrained optimization problems under the above assumptions, and this analysis does not cover more general nonsmooth models or constrained problems. Second, the numerical results may depend on the choices of line search parameters and denoising model parameters, and further adaptive parameter tuning strategies may improve robustness across different classes of problems. Future work will focus on developing adaptive parameter selection rules and investigating accelerated or preconditioned variants to further enhance efficiency on ill-conditioned problems. A dedicated comparison with Perry-type conjugate gradient methods, including the Perry conjugate gradient method and its modified variants, will also be considered, since these methods incorporate quasi-Newton-type curvature information and often demonstrate strong numerical performance in practice. Moreover, extending the proposed framework and its theoretical guarantees to nonsmooth and constrained optimization, as well as to more general imaging inverse problems, remains a worthwhile direction for further research.

Author contributions

Yu Cai conceived the research idea, designed the methodology, developed the proposed algorithms, carried out the theoretical analysis, implemented the numerical experiments, analyzed the results, and wrote the original draft of the manuscript. Hong Yue participated in part of the numerical experiments and assisted with data organization. Chenyun Mo provided general guidance and comments on the

manuscript. All authors reviewed the manuscript and approved the final version.

Use of Generative-AI tools declaration

The authors declare that no AI tools were used in the preparation of this manuscript.

Acknowledgments

This work was supported by Anhui Provincial University Natural Science Research Project (Grant No. 2024AH051658).

Conflict of interest

All authors declare no conflicts of interest in this paper.

References

1. M. R. Hestenes, E. Stiefel, Methods of conjugate gradients for solving linear systems, *J. Res. Natl. Bur. Stand.*, **49** (1952), 409–436.
2. R. Fletcher, C. M. Reeves, Function minimization by conjugate gradients, *Comput. J.*, **7** (1964), 149–154. https://doi.org/10.1093/comjnl/7.2.149
3. E. Polak, G. Ribiere, Note sur la convergence de méthodes de directions conjuguées, *Revue française d'informatique et de recherche opérationnelle. Série rouge*, **16** (1969), 35–43. https://doi.org/10.1051/m2an/196903r100351
4. B. T. Polyak, The conjugate gradient method in extreme problems, *USSR Comput. Math. Math. Phys.*, **9** (1969), 94–112. https://doi.org/10.1016/0041-5553(69)90035-4
5. Y. H. Dai, Y. X. Yuan, A nonlinear conjugate gradient method with a strong global convergence property, *SIAM J. Optim.*, **10** (1999), 177–182. https://doi.org/10.1137/S1052623497318992
6. Y. H. Dai, L. Z. Liao, New conjugacy conditions and related nonlinear conjugate gradient methods, *Appl. Math. Optim.*, **43** (2001), 87–101. https://doi.org/10.1007/s002450010019
7. W. W. Hager, H. C. Zhang, A new conjugate gradient method with guaranteed descent and efficient line search, *SIAM J. Optim.*, **16** (2005), 170–192. https://doi.org/10.1137/030601880
8. Y. H. Dai, C. X. Kou, A nonlinear conjugate gradient algorithm with an optimal property and an improved Wolfe line search, *SIAM J. Optim.*, **23** (2013), 296–320. https://doi.org/10.1137/100813026
9. I. E. Livieris, P. Pintelas, A modified Perry conjugate gradient method and its global convergence, *Optim. Lett.*, **9** (2015), 999–1015. https://doi.org/10.1007/s11590-014-0820-0
10. X. Wang, J. Lv, N. Xu, An improved descent Perry-type algorithm for large-scale unconstrained nonconvex problems and applications to image restoration problems, *Numer. Linear Algebra Appl.*, **31** (2024), e2577. https://doi.org/10.1002/nla.2577

11. Y. Narushima, H. Yabe, J. A. Ford, A three-term conjugate gradient method with sufficient descent property for unconstrained optimization, *SIAM J. Optim.*, **21** (2011), 212–230. https://doi.org/10.1137/080743573

12. Y. H. Dai, Y. Huang, X. W. Liu, A family of spectral gradient methods for optimization, *Comput. Optim. Appl.*, **74** (2019), 43–65. https://doi.org/10.1007/s10589-019-00107-8

13. P. Faramarzi, K. Amini, A scaled three-term conjugate gradient method for large-scale unconstrained optimization problems, *Calcolo*, **56** (2019), 35. https://doi.org/10.1007/s10092-019-0333-4

14. T. Q. Zhang, F. Xue, A new preconditioned nonlinear conjugate gradient method in real arithmetic for computing the ground states of rotational Bose–Einstein condensate, *SIAM J. Sci. Comput.*, **46** (2024), A1764–A1792. https://doi.org/10.1137/23M1590317

15. H. Sato, Riemannian conjugate gradient methods: General framework and specific algorithms with convergence analyses, *SIAM J. Optim.*, **32** (2022), 2690–2717. https://doi.org/10.1137/21M1464178

16. J. K. Liu, S. Q. Du, Y. Y. Chen, A sufficient descent nonlinear conjugate gradient method for solving M-tensor equations, *J. Comput. Appl. Math.*, **371** (2020), 112709. https://doi.org/10.1016/j.cam.2019.112709

17. Z. Aminifard, A. Hosseini, S. B. Kafaki, A modified conjugate gradient method for sparse recovery with nonconvex penalty, *Signal Process.*, **193** (2022), 108424. https://doi.org/10.1016/j.sigpro.2021.108424

18. X. Z. Jiang, W. Liao, J. H. Yin, J. B. Jian, A new family of hybrid three-term conjugate gradient methods with applications in image restoration, *Numer. Algor.*, **91** (2022), 161–191. https://doi.org/10.1007/s11075-022-01258-2

19. K. Wang, D. D. Li, S. H. Wang, A modified RMIL conjugate gradient-based projection algorithm for constrained nonlinear equations: Application to image denoising, *Demonstr. Math.*, **58** (2025), 20250200. https://doi.org/10.1515/dema-2025-0200

20. D. D. Li, J. Q. Wu, Y. Li, S. H. Wang, A modified spectral gradient projection-based algorithm for large-scale constrained nonlinear equations with applications in compressive sensing, *J. Comput. Appl. Math.*, **424** (2023), 115006. https://doi.org/10.1016/j.cam.2022.115006

21. B. M. Khoshsimaye, A. Ashrafi, A family of the modified three-term Hestenes-Stiefel conjugate gradient method with sufficient descent and conjugacy conditions, *J. Appl. Math. Comput.*, **69** (2023), 2331–2360. https://doi.org/10.1007/s12190-023-01839-x

22. A. Yusuf, N. H. Manjak, M. Aphane, A modified three-term conjugate descent derivative-free method for constrained nonlinear monotone equations and signal reconstruction problems, *Mathematics*, **12** (2024), 1649. https://doi.org/10.3390/math12111649

23. M. Rivaie, M. Mamat, L. W. June, M. Ismail, A new class of nonlinear conjugate gradient coefficients with global convergence properties, *Appl. Math. Comput.*, **218** (2012), 11323–11332. https://doi.org/10.1016/j.amc.2012.05.030

24. M. Rivaie, M. Mamat, A. Abashar, A new class of nonlinear conjugate gradient coefficients with exact and inexact line searches, *Appl. Math. Comput.*, **268** (2015), 1152–1163. https://doi.org/10.1016/j.amc.2015.07.019

25. O. O. O. Yousif, The convergence properties of RMIL+ conjugate gradient method under the strong Wolfe line search, *Appl. Math. Comput.*, **367** (2020), 124777. https://doi.org/10.1016/j.amc.2019.124777

26. O. O. O. Yousif, M. A. Saleh, Another modified version of RMIL conjugate gradient method, *Appl. Numer. Math.*, **202** (2024), 120–126. https://doi.org/10.1016/j.apnum.2024.04.014

27. E. G. Birgin, J. M. Martinez, A spectral conjugate gradient method for unconstrained optimization, *Appl. Math. Optim.*, **43** (2001), 117–128. https://doi.org/10.1007/s00245-001-0003-0

28. L. Zhang, W. J. Zhou, D. H. Li, Global convergence of a modified Fletcher-Reeves conjugate gradient method with Armijo-type line search, *Numer. Math.*, **104** (2006), 561–572. https://doi.org/10.1007/s00211-006-0028-z

29. P. Wolfe, Convergence conditions for ascent methods, *SIAM Rev.*, **11** (1969), 226–235. https://doi.org/10.1137/1011036

30. G. Zoutendijk, Nonlinear programming, computational methods, In: *Integer and nonlinear programming*, 1970, 38–86.

31. N. Andrei, An unconstrained optimization test functions collection, *Adv. Model. Optim.*, **10** (2008), 147–161.

32. L. Lukšan, C. Matonoha, J. Vlcek, Modified CUTE problems for sparse unconstrained optimization, Technical Report, 2010.

33. E. D. Dolan, J. J. Moré, Benchmarking optimization software with performance profiles, *Math. Program.*, **91** (2002), 201–213. https://doi.org/10.1007/s101070100263

34. R. H. Chan, C. W. Ho, M. Nikolova, Salt-and-pepper noise removal by median-type noise detectors and detail-preserving regularization, *IEEE T. Image Process.*, **14** (2005), 1479–1485. https://doi.org/10.1109/TIP.2005.852196

35. J. F. Cai, R. Chan, B. Morini, Minimization of an edge-preserving regularization functional by conjugate gradient type methods, In: *Image processing based on partial differential equations*, Berlin: Springer, 2007. https://doi.org/10.1007/978-3-540-33267-1_7

36. X. Wu, X. Ye, D. Han, A family of accelerated hybrid conjugate gradient method for unconstrained optimization and image restoration, *J. Appl. Math. Comput.*, **70** (2024), 2677–2699. https://doi.org/10.1007/s12190-024-02069-5

37. Z. H. Ahmed, M. Hbaib, K. K. Abbo, A modified Fletcher-Reeves conjugate gradient method for unconstrained optimization with applications in image restoration, *Appl. Math.*, **69** (2024), 481–499. https://doi.org/10.21136/AM.2024.0009-24

38. A. B. Abubakar, A. H. Ibrahim, M. Abdullahi, M. Aphane, J. Chen, A sufficient descent LS-PRP-BFGS-like method for solving nonlinear monotone equations with application to image restoration, *Numer. Algor.*, **96** (2024), 1423–1464. https://doi.org/10.1007/s11075-023-01673-z

39. B. A. Hassan, I. A. R. Moghrabi, T. A. Ameen, R. M. Sulaiman, I. M. Sulaiman, Image noise reduction and solution of unconstrained minimization problems via new conjugate gradient methods, *Mathematics*, **12** (2024), 2754. https://doi.org/10.3390/math12172754

40. Z. Wang, A. C. Bovik, H. R. Sheikh, E. P. Simoncelli, Image quality assessment: from error visibility to structural similarity, *IEEE T. Image Process.*, **13** (2004), 600–612. https://doi.org/10.1109/TIP.2003.819861

AIMS Press